SOIL SURFACE ORGANIC LAYERS IN THE ARCTIC FOOTHILLS: DISTRIBUTION, DEVELOPMENT, AND MICROCLIMATIC FEEDBACKS

By

Carson A. Baughman

RECOMMENDED:

David Verbyla
Dr. David Verbyla

Dr. David Valentine

Daniel H. Mann
Dr. Daniel Mann, Advisory Committee Chair

J. Yarie
Dr. John Yarie, Chair
Department of Forest Sciences

APPROVED:

Stephen D. Sparrow
Dr. Stephen Sparrow, Dean
School of Natural Resources and Agricultural Sciences

John C. Eichelberger
Dr. John Eichelberger, Dean of the Graduate School

20 December 2013
Date

SOIL SURFACE ORGANIC LAYERS IN THE ARCTIC FOOTHILLS: DEVELOPMENT, DISTRIBUTION AND MICROCLIMATIC FEEDBACKS

A

THESIS

Presented to the Faculty

of the University of Alaska Fairbanks

in Partial Fulfillment of the Requirements

for the Degree of

MASTER OF SCIENCE

By

Carson A. Baughman, B.A.

Fairbanks, Alaska

December 2013

ABSTRACT

Accumulated organic matter at the ground surface plays an important role in arctic ecosystems. These soil surface organic layers (SSOLs) influence temperature, moisture, and chemistry in the underlying mineral soil and, on a global basis, comprise enormous stores of labile carbon. Understanding the dynamics of SSOLs is a prerequisite for modeling the responses of arctic ecosystems to climate changes. Here we ask three questions regarding SSOLs in the Arctic Foothills of northern Alaska: 1) What environmental factors control their spatial distribution? 2) How long do they take to form? 3) What is the relationship between SSOL thickness and mineral soil temperature during the growing season? Results show that the best predictors of SSOL thickness and distribution are duration of direct sunlight during the growing-season, upslope-drainage-area, slope gradient, and elevation. SSOLs begin to form within decades but require 500-700 years to reach steady-state thicknesses. SSOL formation has a positive feedback on itself by causing rapid soil cooling. Once formed, mature SSOLs lower the growing-season temperature and mean annual temperature of underlying mineral soils by 8° and 3° C, respectively, which reduces growing degree days by 78%. How climate change in northern Alaska will affect the region's SSOLs is an open and potentially crucial question.

TABLE OF CONTENTS

Page

LIST OF FIGURES

Page

LIST OF TABLES

ACKNOWLEDGEMENTS

This research was supported by the US Geological Survey Alaska Climate Science Center, National Science Foundation grant ARC-0902169, and the Scenarios Network for Alaska and Arctic Planning. Logistical support in the field came from The Bureau of Land Management's Arctic Field Office. I thank Mike Kunz, Connie Adkins, Pamela Groves, Curt Baughman, Amy Breen, and Nickoli Kalman for their assistance in the field. We thank Ben Gaglioti, Ben Jones, Miriam Jones, Stephen Tooth, Gary Michaelson, Dave Valentine, Dave Verbyla, Daniel Mann, and Chen Liu Ping for technical support and stimulating discussions.

1.0 INTRODUCTION

Soil surface organic layers (SSOLs) are the uppermost, contiguous, organic soil horizons within a pedon. They are comprised of partly decomposed plant material and are underlain by mineral material. On Alaska's North Slope, the treeless tundra region north of the Brooks Range, SSOLs underlie moist acidic tundra, shrub, and alpine heath communities. SSOLs exceeding 30-40 cm in total depth are classified as peat (Gorham, 1991).

Similarly to peat, SSOLs develop when aboveground primary production exceeds belowground decomposition. This is most commonly due to waterlogging, which causes anoxic conditions that slow decomposition rates (Gorham, 1957). Cold soil temperatures also promote the accumulation of organics (Bonan and Shugart, 1989). At higher latitudes, mean annual soil temperatures (MASTs) near 0° C promote SSOL accumulation by giving plants and the soil surface environment a "thermal advantage" over belowground decomposers (Swanson et al., 2000). Local variations in moisture content and temperature occurring at sub-meter spatial scales are typically the critical factors in determining the outcome of the mass balance between the fixation of carbon and its decomposition.

SSOLs play important roles in tundra ecosystems, including the thermal, hydrologic, nutrient, and carbon-cycling regimes of soils (van Cleve et al., 1986). During arctic summers, SSOLs insulate and promote the persistence of underlying permafrost by virtue of their low thermal conductivity relative to underlying mineral soils (Bonan and Shugart, 1989). SSOLs have high water holding capacity compared to mineral soils, and this property, in conjunction with shallow active layers, is conducive to waterlogging conditions (Hinzman et al., 1991). The combined effect of cooling and waterlogging lowers soil pH, restricts nutrient availability, and

adversely affects plant growth (Beringer et al., 2001; Gorham, 1957; Walker et al., 1994; Walker et al., 2001). Because of their organic nature, SSOLs contain large amounts of carbon and, if decomposed under certain conditions, produce significant amounts of methane (MacDonald et al., 2006). On a circumboreal basis, SSOLs contain an estimated 191 Pg of carbon, which is approximately 6% of the total, global belowground organic carbon pool (Tarnocai et al., 2009). The North American Arctic accounts for approximately ten percent of this SSOL carbon pool (Ping et al., 2008). The contribution of SSOL-derived carbon to underlying mineral soils through cryoturbation, leaching, and other translocation processes has enriched northern soils with carbon to the point that even though high latitude soils only make up 16% of the global soil area, they contain 50% of the global belowground carbon pool (Tarnocai et al., 2009).

Despite the functional importance and ubiquitous nature of high latitude SSOLs, there are major gaps in our understanding of their formation and function (Beringer et al., 2001). Previous studies have described soil formation and soil properties in arctic Alaska (Hobbie et al., 2000; Johnson et al., 2011; Ping et al., 2008), but these are generally large-scale interpolations made at the scale of ecoregions and are based on soil characteristics taken from a statewide data set (Michaelson et al., 2013). SSOL form and function are often lumped into discussions of soil active layers (Johnson et al., 2011; Ping et al., 2008). Furthermore, soil age is often summarized as time-since-deglaciation, neglecting the influence of contemporary disturbance events.

A more precise understanding of SSOL form and function is needed due to anticipated climate warming and the need for more precise landscape models. Mean annual surface temperatures within the Arctic are expected to rise by as much as 7 °C by the end of the century (IPCC, 2007). If we could estimate SSOL thickness and distribution based on environmental

parameters, then we could better predict how ongoing climate changes will affect SSOL-related soil characteristics including carbon stocks at the spatial scale of landscapes (10-100 km).

In other parts of the world, extensive work has been done developing predictive models of soil horizons and peat based on terrain and/or vegetation attributes. For instance, solum depth and A-horizon depth were successfully modeled in southeastern Australia based on topography (Gessler et al., 1995). Similarly, slope angle was used to model mineral horizon thickness in Taiwan (Tsai et al., 2001). Graniero and Price (1999) successfully modeled bog and heath plant community occurrences within a blanket bog using simple terrain parameters, and peat volume and carbon stores have been accurately estimated in the Dartmoor in southwestern England using terrain characteristics (Parry et al., 2012). The ability to remotely predict soil characteristics in this manner saves time and money compared to ground-based soil-surveys (Tsai et al., 2001).

The work described here represents the first attempt at developing a predictive model for SSOLs in arctic Alaska. We utilize multiple study sites within Alaska's central Arctic Foothills (Fig. 1) where SSOLs are ubiquitous and their thickness varies in response to different combinations of terrain, substrate, geomorphic processes, and time. We ask the following questions:

1. **What quantitative, topography-based parameters best correlate with SSOL thickness within the Arctic Foothills? Based on these relationships, what does the distribution of SSOLs tell us about belowground carbon stocks in the study area and region?**
2. H**ow long does it take SSOLs to form on a newly created geomorphic surface? Specifically, how many years are required for a steady-state SSOL to develop?**

3. **What is the relationship between SSOL thickness and belowground temperature? Are there significant temporal thresholds with respect to SSOL thickness and soil temperature?**

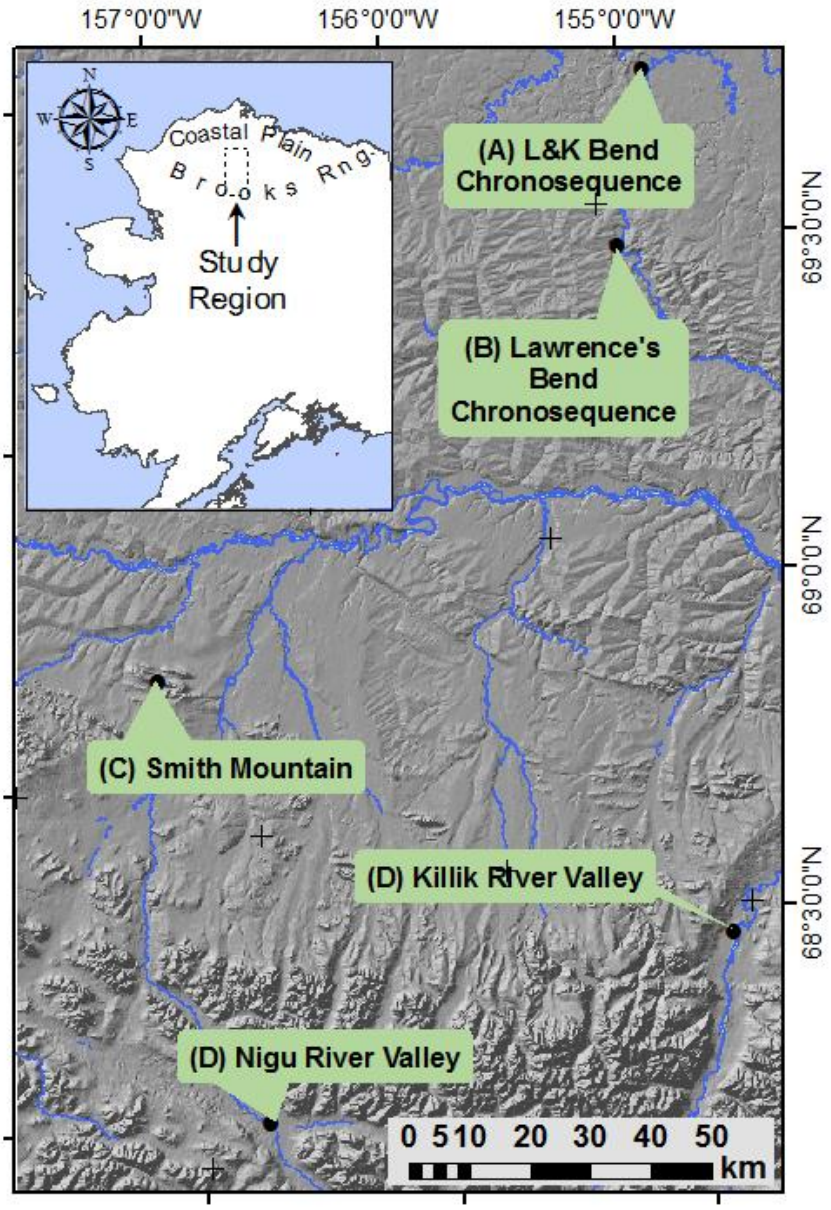

Figure 1. Map of study area.

2.0 REGIONAL SETTING

The Arctic Foothills lie between the Brooks Range and the Arctic Coastal Plain (Fig. 1). Intense folding and subsequent erosion of sedimentary bedrock has produced east-west trending ridges separated by gentle terrain now largely covered by low-, erect-shrub, and moist acidic tundra (Walker, 2000). The foothills closest to the Brooks Range experienced four glacial advances between 1.2 x 10^6 and 10,000 years ago; the most recent occurring between 30,000 and 13,000 years ago (Briner and Kaufman, 2008). The foothills lying north of the Colville River have never been glaciated and consist of expansive rolling topography with few bedrock outcrops and vegetation consisting of erect dwarf-shrub, low-shrub tundra, and moist acidic tundra (Walker et al., 1989; Walker, 2000). Throughout the Arctic Foothills, tundra is the dominant land cover. Sedge-dominated water tracks are common on many low-angle hill slopes, and willow shrubs form gallery thickets along creeks and rivers.

Tundra within the Arctic Foothills is broadly classified as moist acidic tundra or moist nonacidic tundra. Soils within moist acidic tundra are Gelisols, and include Typic, Rupic, and Histic Aquaturbels, Typic Mollihaplels, Typic Molliturbels, and Typic Histohaplels. Soils associated with moist nonacidic tundra consist of Typic Aquaturbels, Typic Histoturbels, and Typic Histohaplels (Bockheim et al., 1998; Ping et al., 1998). These poorly drained, shallow soils dominate the broad sloping valleys, basins, low hills, and foot slopes. They have developed in a mixture of pebbly colluvium and loess-derived silt (Rieger et al., 1979).

The climate on the Arctic Foothills is cold and relatively dry, and the active layer (the upper layer of the soil that thaws and refreezes every year) is generally <1 m in depth. Mean annual precipitation amounts to 14-19 cm, and total winter snow accumulation is generally 70-100 cm.

Typically, July and August are frost-free months, though frost can occur any month of the year. Average maximum summer temperatures are 11-15 °C (Nowacki et al., 2001).

The Arctic Foothills are an ideal location to investigate SSOL distribution, development, and function because the combination of variable topography and high latitude produces a wide range of growing conditions with respect to available light and water. In addition, meandering rivers have produced soil chronosequences where vegetation, soil, and permafrost formation can be observed over time in conjunction with SSOL development. Recently stabilized mass movements (landslides) offer places to compare SSOL-free and SSOL-covered soil environments where belowground temperature regimes can be monitored. The remote location of the study areas provides an opportunity to study natural systems that are largely free of human impacts, unlike many human impacted SSOL-rich landscapes (Holden & Connolly, 2011).

3.0 STUDY SITES

3.1 Smith Mountain

We used the complex topography of the Smith Mountain massif to develop a predictive model of SSOL distribution. Smith Mountain is located 300 km west of the Dalton Highway and 300 km south of Point Barrow (Fig. 1, C). Smith Mountain consists of a sandstone syncline similar to other large east-west running ridges in the Fortress Mountain Formation (Molenaar et al., 1988). The massif has never been glaciated due to its distance from the Brooks Range (40 km). Smith Mountain consists of three prominent ridges dissected by small creeks, Medial Creek being the largest. Kingak Mountain is the highest point on the massif at 638 m above mean sea level

(MAMSL), while the lowest point is at 381 MAMSL. Slope angles are gentle (0-5°) in the lowlands but reach 50° at higher elevations. Incident sunlight varies dramatically between north and south faces, and the complex topography creates striking gradients in soil moisture. The combination of these factors produces a spectrum of growing conditions ranging from dry to wet and from sunny to shady in myriad combinations.

3.2 Ikpikpuk River Soil Chronosequences

Migrating point bars of the Ikpikpuk River (Fig. 1) have created soil chronosequences useful for determining the rate of SSOL development. The Ikpikpuk River is a low gradient, meandering stream with a predominantly sand and gravel bedload that drains a 4,400 km^2 watershed. Its annual mean discharge ranges between 11 and 29 $m^3 s^{-1}$ with no flow occurring between December and April. Peak flow occurs in early June and ranges from 595 to 821 $m^3 s^{-1}$ (National Water Information System, 2013). These break-up floods promote episodic cutbank erosion and meander-scroll formation (Fig 2). Distant from the Brooks Range and lying north of the Colville River, the Ikpikpuk watershed has never been glaciated. Orderly sequences of meander scrolls of varying ages support successional seres extending from newly deposited sand and gravel to SSOL-covered tussock tundra and ice-wedge polygons (Fig. 2).

3.3 Nigu River Landslides

The Nigu River heads in the Brooks Range and flows north into the Arctic Foothills. Its upper valley was glaciated during the last glacial maximum and de-glaciated ca. 14,000 years B.P. (Mann et al., 2010). The present vegetation cover is moist acidic tundra underlain by 5-40 cm of

SSOLs. The valley floor is underlain by thick deposits of outwash gravel containing remnant glacial ice.

Numerous retrogressive thaw slumps (RTSs) (French, 2007) occur along the upper Nigu River and its tributary, Itilyiargiok Creek (Fig. 3). RTSs develop after some sort of initial disturbance exposes permafrost to the atmosphere. Thaw then accelerates and exposes more permafrost. Slump activity is often episodic with several years of quiescence followed by renewed activity. In steep terrain, RTSs can propagate upslope for decades (Lantuit et al., 2012).

Figure 2. L&K chronosequence of meander scrolls deposited by the Ikpikpuk River. Youngest material is deposited on point bar (top-center). Ice wedge polygons have developed on the oldest meander scrolls (bottom-center). River flow (lower-left to upper right) is eroding into old meander scrolls (center).

Retrogressive thaw slumps offer an opportunity to compare soil temperature regimes in early successional conditions with those of undisturbed, “climax”, moist acidic tundra vegetation found immediately outside the slump (Burn and Friele, 1989; Niu et al., 2012). The downslope, distal portions of the slides consist of barren mineral material (Fig. 3) on which soil development begins quickly but proceeds slowly. Physical characteristics such as the accumulation of litter can begin within seven years following slumping, but chemical weathering requires 40+ years (Burn and Friele, 1989). Following stabilization of the slump’s surface, permafrost begins to aggrade (Burns and Friele, 1989) or continues to degrade (Niu et al., 2012).

Figure 3. Retrogressive thaw slump in the upper Nigu valley. Data logging station is in center foreground. Active thaw face in background with intact MAT vegetation and SSOL beyond that. Logging station is enclosed in a cage of hardware cloth to deter animal disturbance.

4.0 METHODS

4.1 Topographic controls over SSOL thickness

We used multiple linear regression (MLR) to investigate the relationships between topographic parameters and SSOL thickness. This method has proved useful for identifying key processes contributing to soil formation and thereby provides context for developing hypotheses about soil-landscape function (Gessler et al., 2000). We chose topographic parameters based on their potential influences on water availability and soil temperatures and calculated their values for every location within the study area using a 5-m resolution SAR-based DEM and ArcMap's® spatial analyst tools. Parameters included slope, aspect, relative elevation (altitude of the point of interest minus the minimum altitude within the Smith Mountain area), upslope-drainage-area, profile curvature (curvature of slope parallel to the direction of the maximum slope), plan curvature (curvature of slope perpendicular to the direction of the maximum slope), curvature (combination of profile and plan curvature), accumulated direct solar radiation, accumulated diffuse solar radiation, and relative duration of direct incoming solar radiation (the amount of hours greater than or less than the average duration of direct radiation experienced over the whole study area). All radiation parameters are based on bi-hourly estimates of incoming solar radiation for May1st – Sept 31st, 2011. We used a 2,800 cell sky size, a 5 day interval, a 2 hour interval, and a standard overcast sky setting for diffuse radiation.

We measured SSOL thickness in the field at 98 locations, termed “model points” arranged along 15 transects situated to span the full range of each environmental parameter within the study area (Fig. 4). At each location, one to four replicate SSOL measurements, termed “sample locations”, were taken. These replicate measurements were spaced 50-100 m apart and were averaged together to calculate mean SSOL thickness values for each of the 98 “model points”. This helped dampen the micro-scale variations in SSOL thickness that are common on organic-rich landscapes (Parry et al., 2012). In the field, the global positioning system was used to navigate to sample locations with an accuracy of ±3 meters. Soil pits approximately 0.1 m^2 in area were

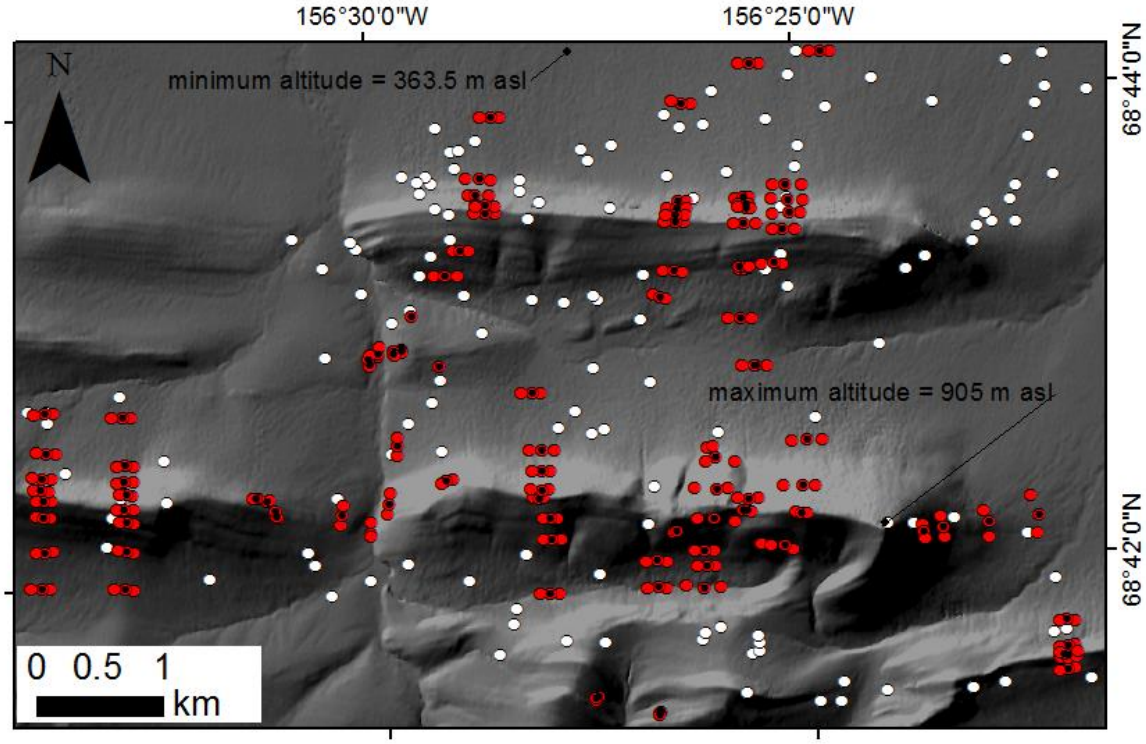

Figure 4. Model points and test pit locations. Model points (black dots, n=98) represent the location of averaged SSOL thickness and parameter values based on the nearest sample locations (red dots, n=281). Test pits (white dots, n=138) are the locations of SSOL thickness measurements used in model assessment.

excavated using hand tools to the depth of mineral soil. SSOL thickness was measured as the distance between the bottom of living moss and the upper surface of the uppermost mineral horizon. A-horizons were considered mineral horizons and were differentiated from overlying organics by color change and increased mineral content. Additionally, we sampled 138 randomly located but predetermined "test pits". Data from these locations were reserved for model testing.

Before inclusion in the MLR, parameters were tested for colinearity by regressing each parameter against the remaining pool of parameters and calculating the variance inflation factor ($VIF = 1/(1-R^2)$) for each regression. In general, the parameter with the highest VIF score (i.e. the one most correlated with all other parameters) was removed from the pool and this process was reiterated until all VIFs were less than 3.0 (Zuur et al., 2010). We maintained parameter diversity by eliminating some parameters whose VIF values were similar but slightly less than the highest VIF score. For instance, we removed one of two radiation-based parameters instead of a lone curvature-based parameter despite the curvature parameter having a slightly higher VIF value.

All sufficiently uncorrelated parameter data (VIF score < 3.0) were combined with their associated SSOL thicknesses and included in the MLR. Backward elimination was performed until all parameters were significant (p-value < .05). The resultant regression equation was then incorporated into ArcMap® to calculate SSOL thickness for every 5m x 5m cell within the study area. We then smoothed this initial SSOL thickness raster to reduce the magnitude of anomalous cells and to give the model output a more natural appearance (ESRI, 2011). To do this, we used the filter tool in the ArcMap® spatial analyst tool box. This tool traverses a 3x3 filter over the entire raster in which every cell is prescribed the mean value of the 3x3 cell matrix that surrounds

it (ESRI, 2011). Finally, the model was tested by comparing observed SSOL thickness with predicted SSOL thickness for each of the 138 test pits.

Following model validation, we developed two pedotransfer functions to estimate regional carbon stocks in the Smith Mountain study area based on the predicted thickness of the SSOL layer. Pedotransfer functions are simply statistical relationships between soil characteristics. Often, complex characteristics are estimated based on more easily measurable properties (Bouma, 1989). They can also be used to estimate missing data within soil surveys based on data that is included (Michaelson et al., 2013). We use two functions to estimate two pools of carbon based on the predicted thickness of the SSOL: 1) the carbon stocks found strictly in the SSOL within the study area and 2); the carbon stocks within the uppermost 1 m of the ground within the study area.

4.2 Timing of SSOL development along the Ikpikpuk River

Two river bends with well-organized meander scroll chronosequences were identified using remote sensing and informally named Lawrence's Bend (LB) and L & K Bend (L&K) (Fig. 1, A, B). Extensive series of meander scrolls indicate prolonged histories of point bar migration (Nanson 1980). To determine how long it takes a SSOL to develop, we first established the age of each chronosequence, then measured SSOL thickness along transects extending from the river bank (*time*=0) inland across progressively older meander scrolls to areas now occupied by ice-wedge polygons and moist acidic tundra. This allowed us to compare SSOL thickness data to estimates of surface age.

We obtained radiocarbon (^{14}C) dates on dead, buried, in-growth-position willow shrubs preserved in and excavated from eroding cutbanks. These shrubs colonized what was once a newly formed point bar but later were buried by overbank sediment and still later by SSOL. The radiocarbon age of a willow represents the latest possible date that the point bar stabilized and hence, how old the geomorphic surface is. We converted radiocarbon dates to calibrated years BP using the Calib 6.0 program (Stuiver & Reimer 1986) and added 60 to the cal yr BP age so we can report chronosequence ages as "years old" with respect to 2010 CE.

At LB, we dug soil pits every 10 meters along the 350 meter long transect (Fig 5) in mid-July 2011. Additional soil pits were dug at the 628, 1117, and 1,270 meters mark. At L&K, we dug soil pits every 5 meters over the first 540 meters of the transect and every 10 meters over the next 380 meters in early July 2012 (Fig. 5). In each pit, the depth of the SSOL was measured to the nearest centimeter. Depth-of-thaw was measured to the nearest cm using three random probes of a tile probe within a 1-meter radius of each soil pit. Shrub canopy height, canopy structure, understory species composition, and the relative dominance of different plant species were recorded at each sampling site.

Every meander-scroll sequence develops through time along a different curvilinear trajectory. This means that the straight-line distance from the currently active point bar is not a useful spatial measurement. A more meaningful metric is the relative position of each data point with respect to the *primary accretion axis* of the scroll sequence (Hicken, 1974). The primary accretion axis reflects the long term growth pattern of the system, and it is defined as the point on each meander-scroll where the orthogonals to the scroll crests can be divided approximately bilaterally (Hicken 1974).

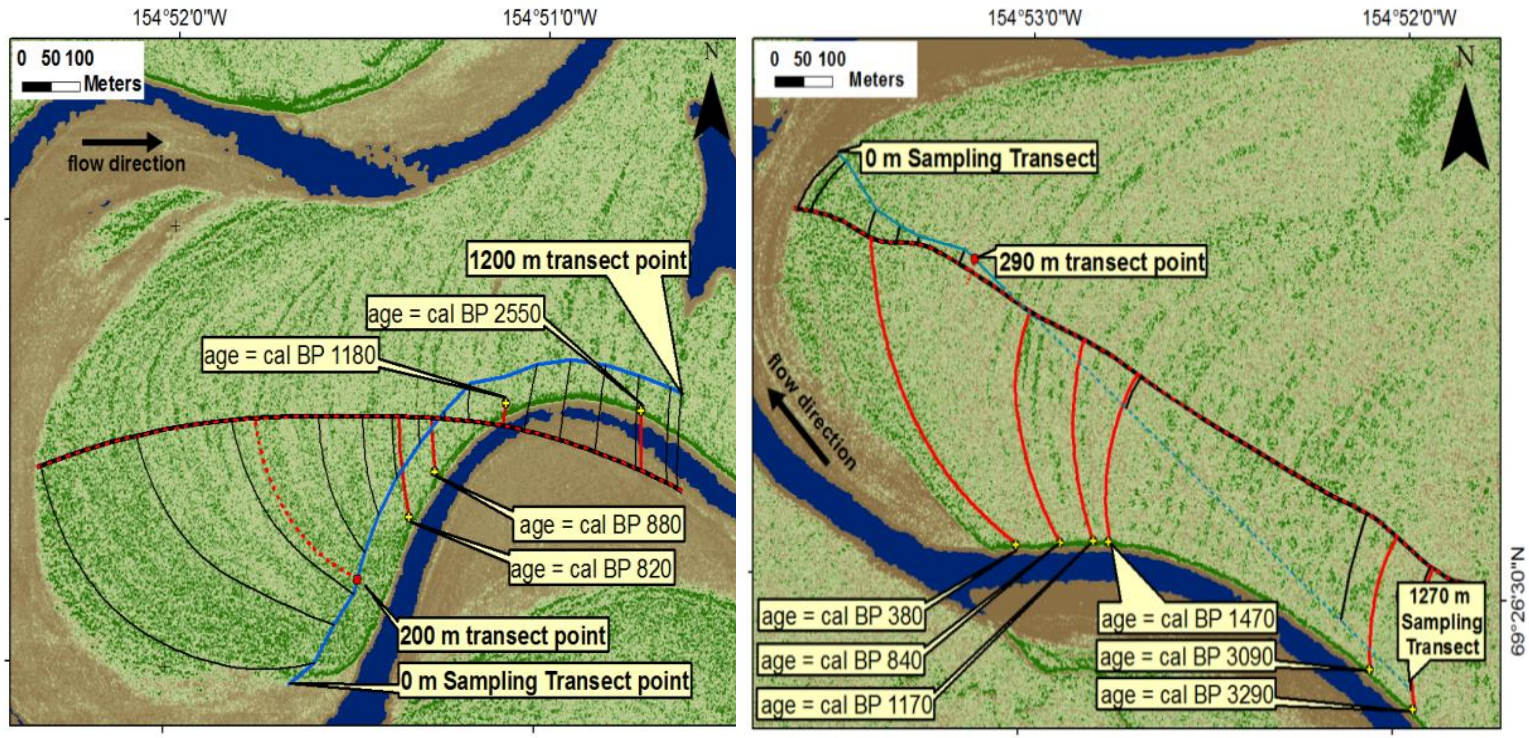

Figure 5. Sample design at L&K chronosequence (top) and Lawrence's Bend chronosequence (bottom). Soil sampling points came from sample transects (blue line). ^{14}C locations (yellow dots) were collected along cutbanks. Location of soil samples and ^{14}C sample sites are projected onto the primary accretion axis (segmented line) using visually determined projection arcs (black or red lines, respectively) based on meander –scroll patterns. A simple linear interpolation equation is used to convert all the distances along the sample transect into distances along the primary accretion axis. The CLAM software program (Blaauw, 2010) is used to infer ages for the intervening positions along these accretion axes.

Once the accretion axis was defined, we projected all sample data onto the axis. To assign ages to specific points along this axis, we traced the scroll ridges and swales under which the dated willows originated laterally to where they intercepted the primary accretion axis. The same was done for a number of reference points along the sampling transect. CLAM version 2.1 software (Blaauw, 2010) was used to infer ages for successive positions along the accretion axis, while a simple linear interpolation equation was used to convert all the remaining distances along the transect to distances on the accretion axis. The end result is a chronosequence in which surface ages are paired with SSOL thicknesses.

4.3 Influence of SSOL development on belowground temperature

To investigate how the presence of a SSOL affects belowground temperature regimes, we measured air and soil temperature for one year at multiple locations of SSOL-free, SSOL-developing, and SSOL-covered sites. Six retrogressive thaw slumps in the Nigu River valley, one blowout in tundra-covered sand dunes along the Killik River, and the Lawrence's Bend point bar provided 9 locations of SSOL-free mineral soil on low elevation, low angle terrain. A total of 16 SSOL-covered sites were instrumented. These consisted of moist acidic tundra immediately adjacent to each of the six retrogressive thaw slumps in the Nigu valley, tundra adjacent to the sand blowout, five vegetated scroll bar surfaces along the chronosequence at LB, and four low lying, low angle moist acidic tundra covered locations on each cardinal flank of Smith Mountain.

Each site was instrumented with two 8K-UA-001-08 HOBO Pendant® Temperature/Alarm data loggers that recorded air and soil temperature bi-hourly. These loggers have a reported accuracy of ± 0.53 °C from 0 to 50 °C and a recommended operating range of -

20 to 70 °C. Temperatures at the retrogressive thaw slumps, blow-out, and point bar sites were recorded for one year (June 2011 – August 2012), while temperatures at the Smith Mountain sites were recoded for June, July, and August, 2012. At SSOL-covered sites (n=16), air temperature was recorded 8-10 cm above the moss surface while soil temperature was measured at the organic/mineral interface. At SSOL-free locations (n=9), air temperature was measured 8-10 cm above the soil surface and soil temperature was measured 2-4 cm below the ground surface. At Lawrence's Bend, we measured air and soil temperature under SSOL-free, SSOL-developing, SSOL-established, and climax SSOL conditions. The 20, 40, 100, 150, 190, 270, and 1,200 m locations along the LB sampling transect were instrumented with data loggers and air and soil temperature was recorded bi-hourly with the same focus on the mineral/organic interface. At every location throughout the study, two sets of temperature loggers were used for replicate measurements and were typically 10-20 m apart.

5.0 RESULTS

5.1 Distribution of SSOLs on Smith Mountain

We found mean SSOL thickness to be 8.0 cm with a standard deviation of 5.6 cm. Minimum and maximum observed SSOL thicknesses were 0 and 26 cm, respectively. SSOL-free areas generally occurred on steep slopes (>40°), ridge tops, scree fields, and in areas disturbed by ground squirrel and bear diggings. The thickest SSOL (26 cm) occurred on a north-facing, 25° slope on the western edge of the study area. All but one other SSOL thickness >20 cm occurred on slopes less than 10°-20°. Every model point consisted of one (n=2), two (n=10), three (n=85), or

4 (n=1) sample locations. Shallow depth-of-thaw at the time of measurement made it difficult to measure the maximum SSOL thickness at 23 (8% of) sample locations. These locations were shared between 15 model points. Of these 15 points, only in one case were we unable to reach the bottom of the SSOL in any of the replicate sample locations.

For MLR construction, all parameters were sufficiently normally distributed except *slope* and *up-slope-area*, which were transformed using a square root function (***x*$^{0.5}$**). Topographic parameters that we found to be sufficiently uncorrelated with one another included *duration*, *plan curvature*, *up-slope-area*$^{.5}$, *relative elevation*, *aspect*, and *slope*$^{.5}$. A first-order MLR revealed only *up-slope-area*$^{.5}$ and *relative elevation* to be significant. When cross-product (two-way) interactions were employed, *duration*, *up-slope-area*$^{.5}$, *relative elevation*, and ***(****slope*$^{.5}$**relative duration)* were found to be significant predictors. The latter more complex model was selected over the initial model as it had a higher adjusted R^2-value (0.55 vs. 0.52), smaller residual standard error (3.7 vs. 3.9), and comparable overall F-test p-values (2.2×10^{-16} vs. 2.29×10^{-16}). MLR output from the latter model was used to construct the best-fitting regression equation (Eq. 1).

(Eq. 1) $$Y = -0.01(dur) + 0.79 * flo^{0.5} - 0.026 relelev + 0.003(slope^{0.5} reldur) + 37$$

Where *Y* equals SSOL thickness (cm), *dur* equals duration of direct radiation (hours), *flo* equals up-slope-drainage-area (25 m^2)*, slope* equals slope (degrees), and *reldur* equals duration of direct radiation of the location relative to the study area mean (hours).

Utilization of these parameters produced an overall adjusted R-squared of 0.55 (Table 1). Based on p-values, *up-slope-area*$^{.5}$ **and** *relative elevation* were most significantly correlated with variation in SSOL thickness. The interaction variable ***(****slope*$^{.5}$**relative duration)* is the next most

significant parameter, and *solar duration* is the least significant. An increase in *solar duration* or *relative elevation* accompanies thinner SSOLs while an increase in *up-slope-drainage-area* or the interaction variable accompanies an increase in SSOL thickness.

Table 1. Multiple Linear Regression output with respect to topographic controls of SSOL thickness.

Parameters	**Estimate**	**Std. Error**	**t value**	**PR(>t)**
(Intercept)	36.957	12.485	2.96	0.004
duration	-0.012	0.005	-2.234	0.028
up-slope-drainage	0.793	0.165	4.806	5.97E-06
relative elevation	-0.026	0.004	-5.412	4.93E-07
sqrt(slope)*rel. dur.	0.003	0.001	2.821	0.006

Residuals:	Min	1Q	Median	3Q	Max
	-9.8	-2.2	-0.3	2.2	9.1

Multiple R-squared: 0.578

Adjusted R-squared: 0.5551

F-statistic: 25.21 on 5 and 92 DF

p-value: 6.35e-16

5.2 SSOL Thickness Modeling and Validation

The best-fitting regression equation (Eq. 1) was incorporated into ArcMap® and used to predict SSOL thickness in every 5m x 5m cell within the study area. Five iterations of smoothing reduced the majority of anomalous cells. The resulting SSOL thickness raster predicted a range of SSOL thicknesses from -12.4 to 64.8 cm. To produce a final SSOL thickness map, all negative values were reclassified to zero, and all values were rounded to the nearest centimeter (Fig. 6). Mean

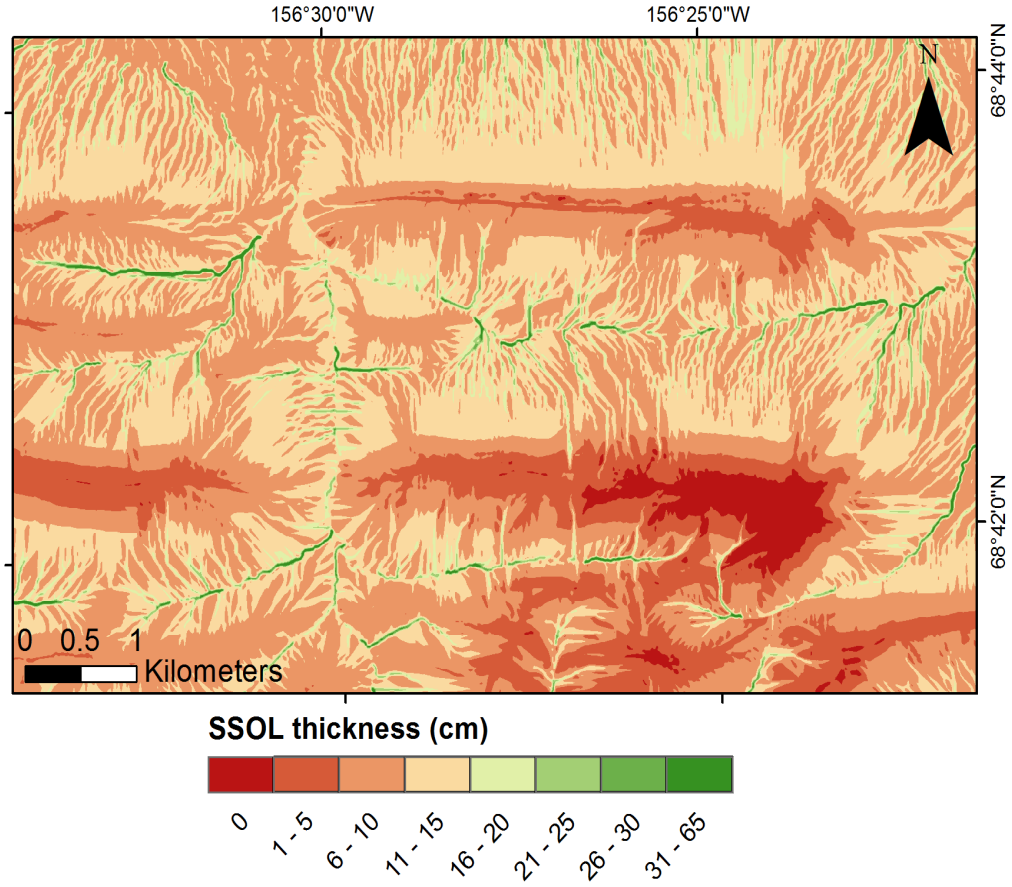

Figure 6. Model estimates of SSOL thickness. SSOLs >17-18 cm are restricted to water tracks. The thickest SSOLs occur where water tracks converge to form first order drainages. SSOLs are absent or thin on ridge tops, steep slopes, and at high elevations.

SSOL thickness for the study area was 10.0 cm with a standard deviation of 4.7 cm. Minimum and maximum SSOL thickness was 0 and 64 cm, respectively.

Model testing found moderately strong agreement between the predictions and observations (Fig. 7) with 14% of predictions matching observed thicknesses exactly, 50% of predicted values falling within 3 cm or less of their observed thicknesses, and 78% falling within 5 cm or less. The model appears to over-predict the occurrence of thin SSOLs (<12 cm) and under-predict thick SSOLs (> 12 cm). In some cases, the model predicts SSOLs where we observed there to be none, usually estimating there to be 1-5 cm of SSOL present. In general, the model underestimates regional SSOL volume. We observed a total of 1,572 cm of SSOL when all 138 test pit SSOL thicknesses were summed, whereas the model predicted a total of 1,487 cm, which was slightly less than observed.

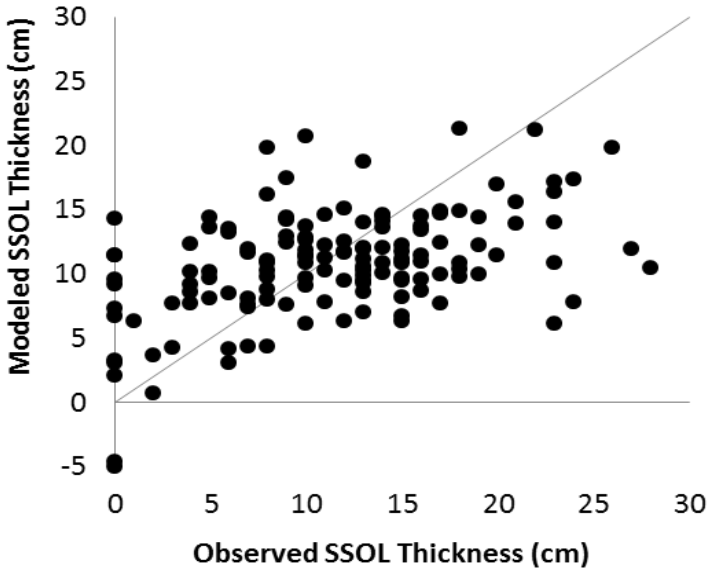

Figure 7. Observed vs. modeled total SSOL thickness. The model is biased in overestimating SSOL thickness for SSOLs less than 11 cm and biased in underestimating SSOL thickness for SSOLs greater than 11 cm.

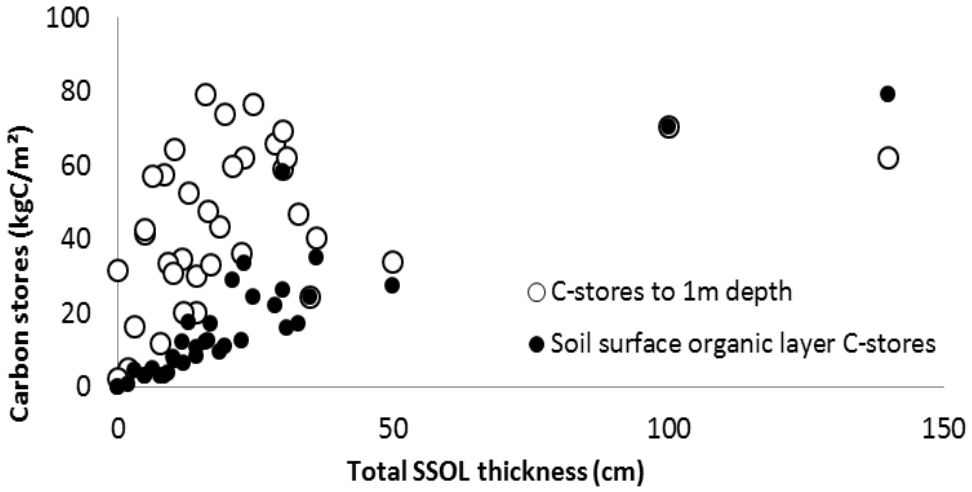

Figure 8. Relationship between SSOL thickness and carbon stocks. SSOL-contained carbon stocks are solid circles while total soil carbon stocks to one meter depth are open circles. N=36 soil pits within the Arctic Foothills (redrawn using data from Michaelson et al., 2013).

5.3 Inferring carbon stocks from modeled SSOL thickness

A close relationship exists between SSOL thickness and SSOL-based carbon stores in the Arctic Foothills (Fig. 8, Eq. 2) due to the regional uniformity of bulk density within surficial organic layers (Michaelson et al., 2013). The relationship between SSOL thickness and carbon stores to 1 meter depth is weaker and probably not accurately quantified due to the limited number of sample soil pits and the geomorphic diversity of their locations (Fig. 8, Eq. 3). These relationships

are based on an Arctic-Foothills-subset (n=36) of the most recently cataloged University of Alaska and USDA-NRCS soil profiles (Michaelson et al., 2013).

Applying equations 2 and 3 to the SSOL thickness model output results in an overall estimate of 1.9 ± 0.52 teragrams (Tg) of carbon for the 47 km^2 Smith Mountain area (± = 95% c.i.). This equates to 40.5 ± 11.02 kg C m^{-2}. Carbon stocks are partitioned unequally, with 17% (0.32±0.04 Tg) occurring within SSOLs and the remainder in the underlying mineral soil to a depth

(Eq. 2) $SSOL\ kgC/m^2 = 0.68(SSOL\ thickness)\quad r^2=0.88,\ n=36$

(Eq. 3) $1\text{-}meter\ depth\ kgC/m^2 = 0.29(SSOL\ thickness) + 37.8\quad r^2=0.14\ n=36$

of 1 m. SSOL-based carbon stocks ranged from 0 to 44 kgC m^{-2} with a mean of 6.7 kgC m^{-2} and a standard deviation of 3.0 kgC m^{-2} (Fig. 9). Estimated 1-meter-depth carbon stocks ranged between 34 and 56 kgC m^{-2} with a mean of 40.3 kgC m^{-2} and a standard deviation of 1.3 kgC m^{-2} (Fig. 9).

5.4 Time to SSOL development

We used the Ikpikpuk chronosequences to estimate how long it takes for SSOLs to form and reach a steady state in a floodplain setting. Six and four ^{14}C dates were obtained along the southern cutbank at Lawrence's Bend and L&K bend, respectively (Fig. 5). The oldest portion of the LB and L&K transects date to approximately 3,300 ± 40 cal yr BP (LB) and 2,510 ± 130 cal yr BP (L&K), respectively (Table 2). Vegetation succession along the chronosequences was similar at both river bends (Table 3). Immediately adjacent to the sandy point-bar, a meadow-like community exists in which vegetation is sparse and bare sand and/or gravel is widely exposed. Vegetation consists of grasses, forbs, and scattered willow bushes. Within the first 100 meters

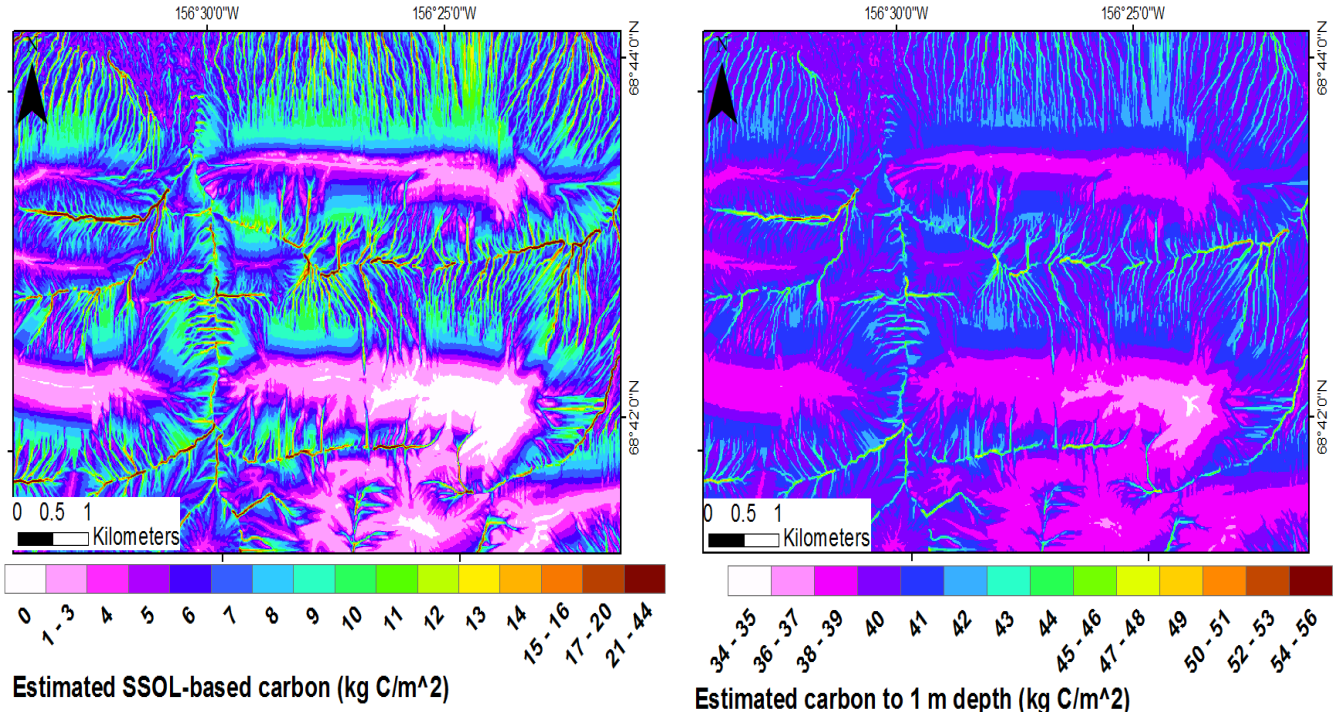

Figure 9. Inferred carbon stocks of Smith Mountain. **Left:** Inferred carbon stocks contained in the SSOL based on kg of carbon per cm thickness of SSOL (*Eq. 2*). **Right:** Inferred carbon stocks contained in the top meter of soil based on kg of carbon per cm thickness of SSOL (*Eq. 3*). Relationship between SSOL thickness and carbon stocks are based on 36 UAF and/or NRCS soil pits within the Arctic Foothills province (Michaelson et al., 2013).

Table 2. Radiocarbon (^{14}C) dates from the Ikpikpuk River

Field number	Lab number Beta-######	Location Lat. (°N), Long. (°W)	Dated Material	$\delta^{13}C$ (°/₀₀)	^{13}C-normalized age (years before 1950 CE)	1 std dev	2s calibrated age range (cal yr. BP)	Mean probable calibrated age (cal yr BP)
Lawrence's Bend								
LBEND14	311696	69° 26.5', 154° 53.0'	willow in growth position (WGP)	-29.0	310	30	301:463	380
LBEND13	315152	69° 26.5', 154° 52.9'	WGP	-27.0	920	30	766:922	840
LBEND12	315151	69° 26.5', 154° 52.8'	WGP	-26.4	1240	30	1077:1264	1170
LBEND11	311695	69° 26.5', 154° 52.8'	WGP	-27.5	1580	30	1403:1535	1470
LBEND03	311694	69° 26.4', 154° 52.0'	WGP	-29.1	2930	30	2973:3208	3090
LBEND01	311693	69° 26.4', 154° 51.9'	WGP	-27.4	3070	30	3215:3362	3290
L&K Bend								
LK17	331699	69° 41.1', 154° 51.3'	WGP	-29.8	900	30	739:910	820
LK16	331696	69° 41.1', 154° 51.3'	WGP	-27.8	1000	30	798:967	1070
LK15a	331698	69° 41.2', 154° 51.1'	WGP.	-27.1	1260	30	1088:1281	1180
LK7a	331697	69° 41.2', 154° 50.7'	WGP	-28.9	2490	30	2368:2725	2550
LK7b	331694	69° 41.2', 154° 50.7'	Basal 2 cm of 20 cm thick peat layer covering LK7a	-28.7	990	30	797:961	880

Table 3. Summary of SSOL development on chronosequences and co-occurring changes in depth of thaw and overlying vegetation through time. SSOL = soil surface organic layers. MAT = moist acidic tussock tundra.

L&K Chronosequence

Estimated Age (years before 2012, 99% c.i.)	SSOL Developmental Stage	Mean July depth of thaw (cm)	Vegetation
0	bare sand	91	None
6±2	first organics	58	tall willow thicket, 100% ground cover of moss.
108±10	proto-SSOL	45	1 m tall willow and alder. Patches of dwarf willow and lupine. 100% moss cover. Scattered forbs.
550±50	mature SSOL	18	0.5 m tall willow shrubs. Sedge, moss and dwarf willow carpet.
3300±40	climax SSOL	16-35	Ice wedge polygons. Polygon centers filled with standing water and sedges. Moist Acidic tundra dominated by *E. vaginatum* and *B. nana*

Lawrence's Bend Chronosequence

Estimated Age (years before 2011, 99% c.i.)	SSOL Developmental Stage	Mean July depth of thaw (cm)	Vegetation
0	bare sand	105+	None
20±4	first organics	105+	Sand bar with scattered herbaceous perennials. <5% vegetation cover. Large solitary willow. Signs of annual inundation.
260±50	proto-SSOL	74	Inland side of tall willow thicket. 1-2m tall willow. Moss and dwarf willow carpet. Scattered *Lupinus*, A*staralus sp.* And grasses
720±60	mature SSOL	24	0.3 m tall willow and dwarf birch. *Eriophorum* tussocks present
2510±150	climax SSOL	16	Well-developed tussock tundra with low-growing willow and *B nana*. Ice wedge polygons nearby.

from the shoreline, willow shrubs form a thicket up to 3 meters in height. Ground cover is still patchy and consists of mosses, *Equisetum*, and forbs. Moving inland, the ridge and swale topography of the meander scrolls produces small- variations in plant communities.On the meander scroll ridges, low stands of willow and ericaceous shrubs occur. There is 100% ground cover consisting of shrubs, mosses, and scattered forbs. Sedges grow in the intervening swales. Still further inland (150 – 170 m), shrub tundra becomes widespread with shrubs rarely exceeding 70 cm in height. This assemblage persists until ice-wedge polygons develop under moist acidic tundra vegetation at the end of each transect.In addition to the changes in vegetation just described, striking changes in soil development, SSOL thickness, and depth of thaw occur along both chronosequences (Table 3). At L&K bend, organic accumulation begins in isolated patches around 45 m inland, which has an estimated age of <10 yr (calibrated years before 2010 CE). These scattered patches of SSOL consist of either moss or herb, grass, and/or willow leaves. A very thin SSOL develops around 85 m inland and consists of thin, alternating bands of buried litter and sediment indicative of periodic flood deposition within swales. This location was estimated to be 110 ± 10 yr (± 1 σ). A continuous O-horizon first appears around 100 m inland, which has an estimated age of 170 ± 10 yr. Simultaneously, depth-of-thaw erratically decreases (Fig. 10). The trend of thickening organics and thinning depth-of-thaw continues until approximately 200 meters from the active point bar where they both reach fluctuating steady states. At this point, where surface age is 550 ± 50 yr old, we consider the SSOL to be "fully formed." Beyond this point, both SSOL thickness and depth of thaw remain relatively constant (Fig. 10).

At Lawrence's Bend, soil organic accumulation follows a similar pattern as at L&K bend (Table 3). Surface organics begin to accumulate 20 meters inland of the bare, active surface of

the point bar. The 20 meter mark is estimated to be 20 ± 4 yr old. A pronounced organic horizon has developed around 70 meters inland, a location estimated to be 260 ± 50 yr old. The depth-of-thaw thins erratically until approximately the 290 meter point where it begins to stabilize. This location is estimated to be 720 ± 60 yr old and represents the point where SSOL reaches a steady state (Fig. 10).

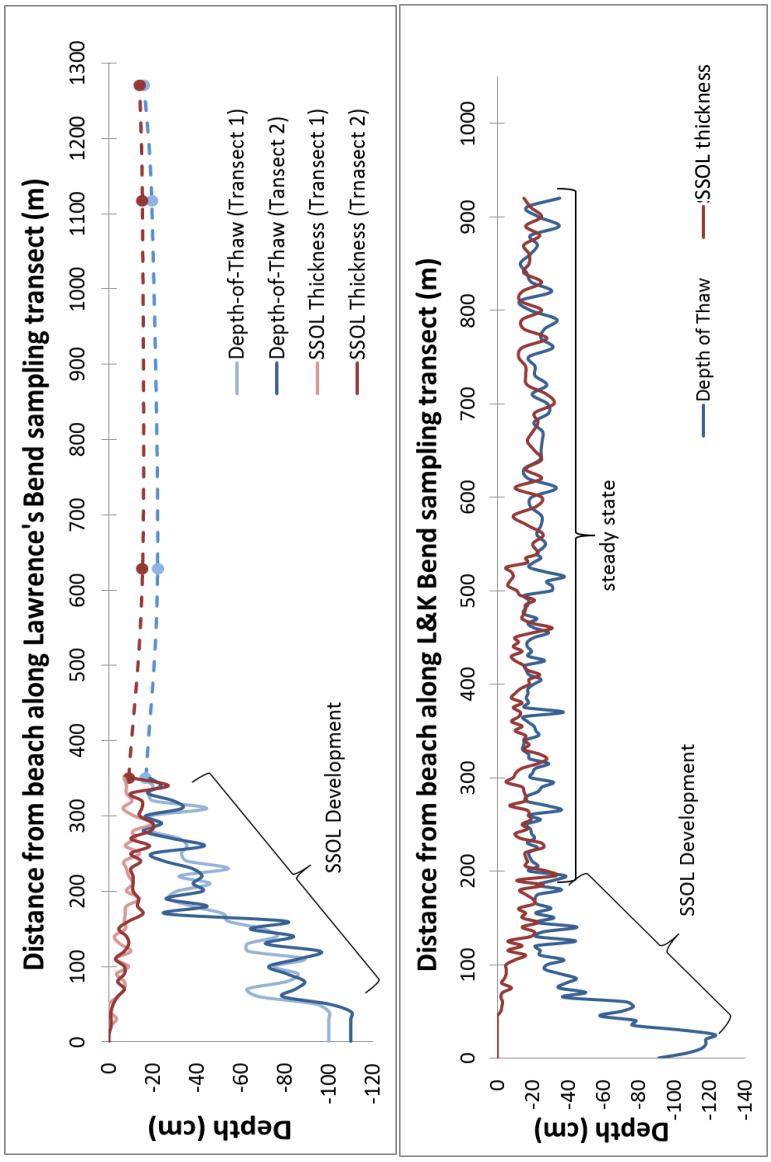

Figure 10. Relationship between SSOL thickness and chronosequence distance from the beach along the sampling transect. SSOL formation initiates rather quickly, stabilizes between 200 m (bottom) and 300 m (top), and maintains a steady-state the remainder of the sampling transect. The first location of steady-state thickness is considered the location where SSOLs are fully formed.

5.5 Feedbacks of SSOL on Soil Temperature

Six of the seven instrument arrays that we installed at SSOL-covered sites in the Nigu and Killik River valleys survived for one year without animal disturbance. At these 6 sites, SSOLs in undisturbed moist acidic tundra had a mean depth of 13 cm with a standard deviation of 2 cm. On Smith Mountain, mean SSOL thickness at the 4 instrumented sites that we monitored over the growing season in 2012 was 17.4 cm with a standard deviation of 1.7 cm. A z-test comparing mean air temperatures within and outside of the five retrogressive thaw slump sites from June

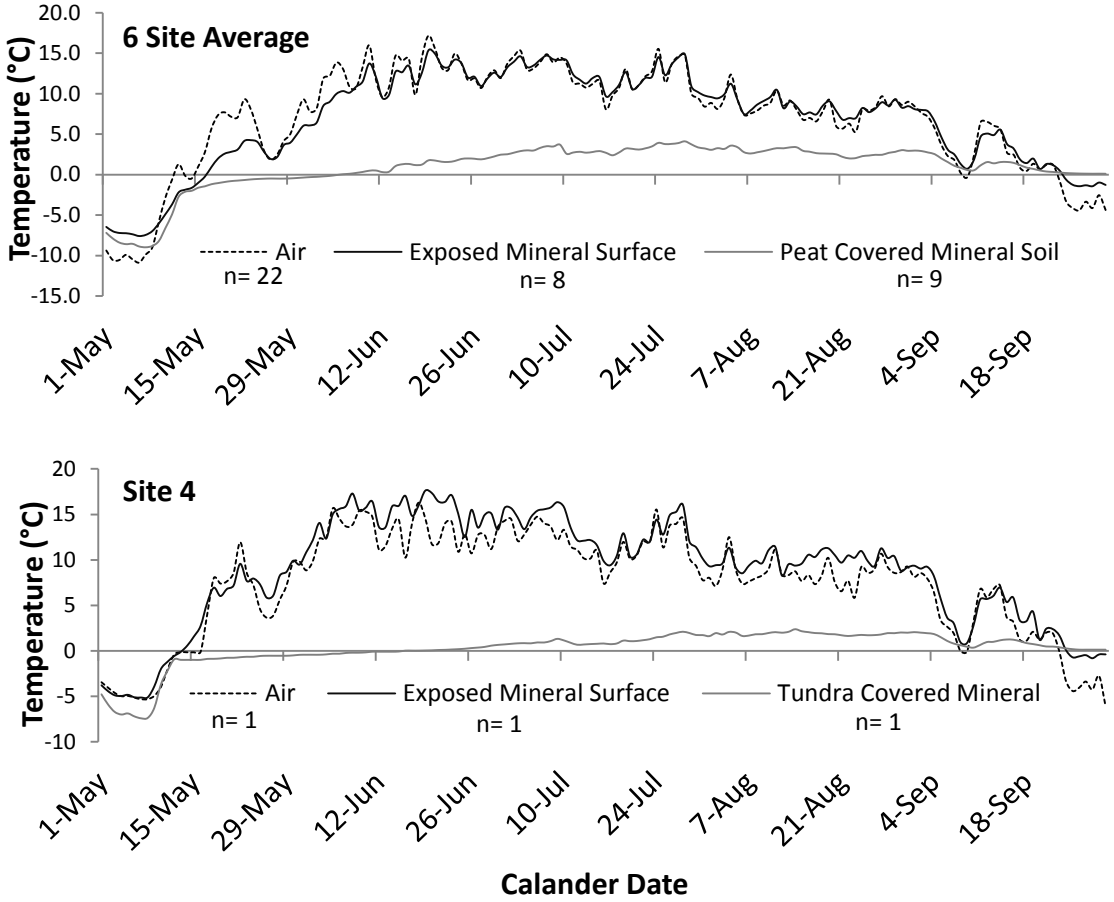

Figure 11. Six site average and individual site temperature profiles. Six site average (top) and individual site (bottom) depict annual temperature profiles through the growing season from Nigu River Valley retrogressive thaw slumps.

through August found no significant difference in their mean temperatures (α=0.01, p-value=0.32). Therefore we assume that differences seen in mineral soil surface temperatures in the undisturbed tundra bordering the retrogressive thaw slumps were caused by the presence of SSOLs (Fig. 11).

We found that the presence of SSOLs is associated with markedly lower monthly mean soil temperature at the organic/mineral interface (Fig. 12, Table 4). June, July, and August mean soil temperatures (MST) were reduced by 10.5 °C, 9.2 °C, and 5.7 °C, respectively. This left June, July, and August MSTs barely above 0°C at 1.2 °C, 3.3 °C, and 2.9 °C, respectively. The presence of SSOLs also lowers both soil temperatures during the peak of the growing season (June-July-August) and mean annual soil temperature (MASTs) by 7.8 °C and 2.9 °C, respectively.

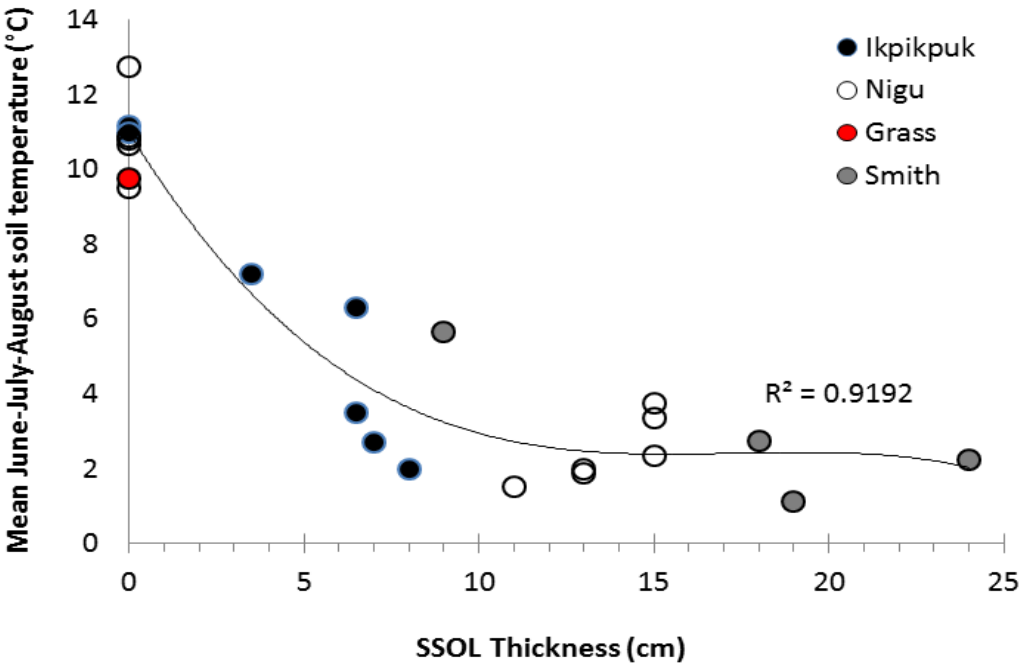

Figure 12. Influence of SSOL thickness on soil temperature. The influence of overlying SSOL thickness on Mean June-July-August mineral soil temperature may indicate a non-linear relationship between increasing SSOL thickness and the cooling of underlying mineral soils.

Temperature measurements from all study sites show that an increase in SSOL thickness strongly correlates with a decrease in mean growing season (JJA) soil temperature (Table 4).

Growing degree days (GDD) at the mineral soil surface were also strongly affected by the presence of SSOLs. Under climax-state SSOLs (i.e., intact, mature tundra vegetation), annual GDDs (accumulated daily mean temperature > 0°C) at the organic/mineral soil interface totaled 263°C compared to 1,142°C at -2cm depth in bare mineral soil (Table 4). This equates to a reduction of available heat energy by 77% (Fig. 13).

Table 4. Summary of air and soil temperature characteristics of SSOL-covered and bare mineral soil. SSOL thickness averages 13 cm. Values based on 5 retrogressive thaw slumps along the Nigu River and 1 canoe-shaped blow-out in sand dunes along the Killik River.

	SSOL-covered	± 1 stdev	**Bare mineral**	± 1 stdev
mean Avg. May Air temp	0.8	0.4	-0.6	0.9
mean Avg. May Soil temp	-3.4	0.1	-0.8	0.6
mean Avg. June Air temp	12.8	0.4	11.9	0.4
mean Avg. June Soil temp	1.2	0.4	11.7	0.7
mean Avg. July Air temp	12.3	0.2	12.3	0.2
mean Avg. July Soil temp	3.3	0.6	12.5	0.3
mean Avg. August Air temp	7.9	0.2	8.4	0.3
mean Avg. August Soil temp	2.9	0.3	8.6	0.4
mean Avg. Sept. Air temp	1.3	0.1	1.9	0.3
mean Avg. Sept. Soil temp	1.1	0.1	2.4	0.3
mean Avg. Oct. Air temp	-7.0	0.8	-4.8	0.4
mean Avg. Oct. Soil temp	-0.1	0.1	-2.2	0.3
mean JJA Air temp	11.0	0.2	10.9	0.3
mean JJA Soil temp	3.2	0.4	10.9	0.5
mean Annual Air temp	-6.8	0.8	-3.4	1.4
mean Annual Soil temp	-4.4	0.1	-1.5	1.0
mean Air Degree Days >0°C	1204.0	30.7	1153.9	47.2
mean Soil Degree Days >0°C	262.6	33.7	1141.9	63.9
mean Thermal Advantage	941.4	50.8	-5.7	92.4

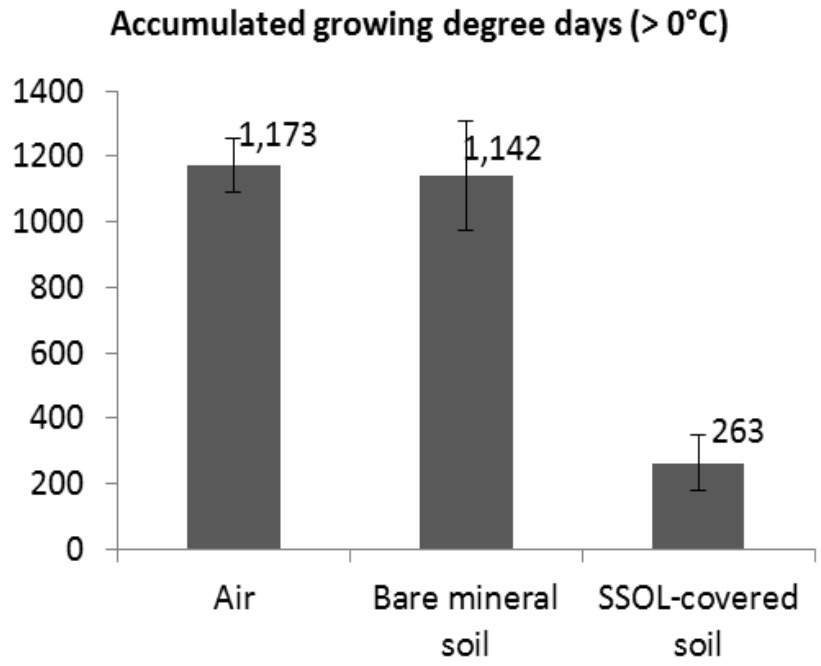

Figure 13. Cumulative Growing Degree Days vs. SSOL coverage. There are similar Cumulative Growing Degree Days (days >0 °C) for air and bare soils. SSOL-covered soils have significantly less growing degree days. Average SSOL thickness = 13+/- 1 cm n = 5.

DISCUSSION

6.1 The Smith Mountain SSOL Model

We found a moderately strong relationship between SSOL formation and topographic parameters (adjusted R^2 = 0.55). This is as good as or better than other soil models whose goal is to predict soil characteristics using terrain parameters. For example, solum depth and A-horizon depth have both been modeled in Australia using regression equations with an associated R^2-value of 0.68 and 0.63, respectively (Gessler et al., 1995). In Taiwan, slope angle was used to model B and B+BC horizon thickness using R^2 values as small as 0.05 and 0.07, respectively, by

Tsai et al. (2001). Working in Labrador, Graniero and Price (1999) modeled bog and heath plant community occurrences within a blanket bog using similar parameters as ours with an R^2 of 0.22. Parry et al. (2012) successfully predicted peat volume and carbon stores on the Dartmoor using R^2-values ranging from 0.27 to 0.54.

Despite moderate or even low R^2-values in the studies mentioned above, each author deemed their model capable of practical application. This is possible because R^2-values alone are not a sole indicator of a predictive model's accuracy (Zuur et al., 2010). The direct comparison of model predictions with reserved sets of validation or test data offer a more incisive assessment of model capabilities. Ultimately it appears that the soil modeling community has accepted a certain degree of fuzziness when modeling the complexity of soil formation. In the words of Gessler et al. (1995); *"The ubiquitous and substantial short range variation of soil attributes places a fundamental limit on the quality of spatial prediction."*

6.2 How realistic are the soil carbon stock estimates?

Our modeling results yields an estimated 6.6 ± 0.8 kg C m^{-2} contained in SSOLs and 40.6 ± 2.6 kg C m^{-2} contained in the soil to a depth of 1 meter within the Smith Mountain study area for a total of 0.32 ± 0.04 Tg and 1.9±0.52 Tg, respectively (± 95% confidence interval). Our SSOL-based carbon stock is likely to be an underestimate of what is actually present. The model predicts a cumulative SSOL thickness of 1,487 cm for the 138 test pits when we actually observed a total of 1,572 cm. Despite this, our estimates of the amount of organic C stored in SSOLs on Smith Mountain are consistent with previous studies that have attempted to quantify belowground C in the Arctic Foothills.

Soil carbon stocks have been previously estimated for the Kuparuk River Basin (Michaelson et al., 1996) and Alaska's "arctic uplands," which include the Arctic Foothills (Johnson et al., 2011). The Kuparuk River Basin lies 200-300 km east of Smith Mountain and encompasses both the Arctic Foothills in its southern reaches and the Coastal Plain in the north. Michaelson et al. (1996) estimated carbon stores within the active layer in the Arctic Foothills portion of the Kuparuk River Basin to be 22 ± 10 kg C m^{-2} (± = standard deviation). Johnson et al. (2011) estimated surface organics within the Arctic uplands using the same state-wide, University, and NRCS soils data set as Michaelson et al. (2013) and estimated the uplands to contain 5.6 to 8.8 kgC m^{-2}. Our estimates of SSOL carbon on Smith Mountain fall within these previous estimates. Those of Michaelson et al. (1996) are higher than those of both Johnson et al. (2011) and ours because Michaelson et al. (1996) estimate carbon stores for the entire active layer (Johnson et al., 2011; Ping et al., 2008; Tarnocai et al., 2009). These rich accumulations of sub-SSOL organics often occur as cryoturbated organic matter that has accumulated at the base of the active layer (Bockheim, 2007).

The fact that our model slightly underestimates SSOL volumes in the study area while providing reasonable estimates of regional carbon densities seems slightly contradictory; however, this is because of the model's tendency to predict thicker SSOLs than were actually observed in the study area. This is not a failure of the model, since SSOLs in excess of 30 cm likely do exist within the study area based on observations of peat accumulations exposed along regional river cutbanks and in auger holes bored in a nearby watershed.

Equation 3 probably overestimates the amount of organic C stored in the upper meter of the ground on Smith Mountain. This is because large portions of the soils on Smith Mountain are

Inceptisols (shallow, weakly developed soils over unconsolidated material) immediately underlain by bedrock. These soils would not be able to incorporate much carbon via cryoturbation. The large value of 40 ± 2 kg C m^{-2} is simply a product of the relationship found between SSOL thickness and 1-meter deep carbon stores from what are diverse and in some cases quite different geomorphic settings in the Arctic Foothills (Mishra and Riley, 2012) (Eq. 3). This estimate could be improved with additional, concerted soil-pit excavation and sampling.

6.3 Timing of SSOL Development

On the floodplain of the Ikpikpuk River, organic matter begins to accumulate at the ground surface within several decades of point bar stabilization. These organics accumulate to form a SSOL whose thickness reaches a steady state after 500 to 700 years. Our data show that SSOL accumulation occurs rapidly at first and then slows (Fig. 14). The high degree of spatial variability seen in climax-state SSOLs is due to small-scale topographic features created by meander scroll topography and later by ice wedge polygons. In swales, SSOLs develop quickly and thicken rapidly through time; on scroll crests, SSOLs are slower to form and remain relatively thin there. Microtopography is an important factor in controlling SSOL development within these floodplain chronosequences just as it is on the slopes of Smith Mountain.

It is important to note that carbon within a SSOL is constantly cycling, so that a SSOL's basal ^{14}C age can be significantly younger than the age of the underlying geomorphic surface. For instance, a location along the L&K chronosequence that dated to 2550 yr based on the age of a willow buried in the underlying sediment was capped by 20 cm of SSOL whose basal 2 cm of

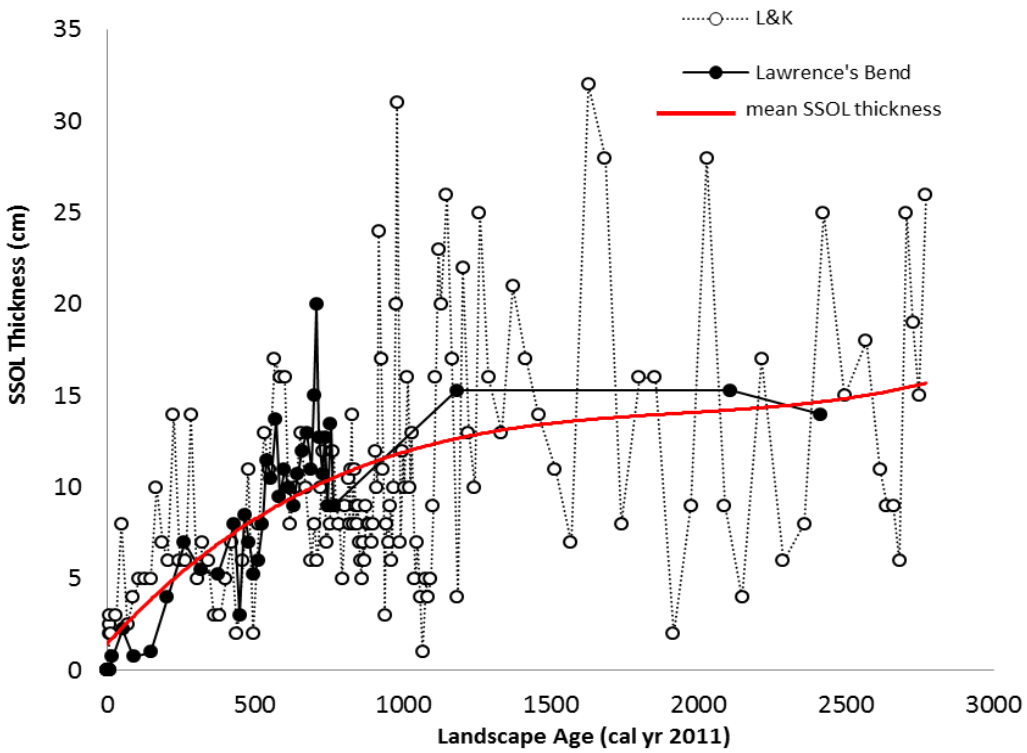

Figure 14. SSOL depth with respect to estimated landscape age. While the first 500-700 years are fairly constrained, SSOL thickness over older geomorphic surfaces varies widely. In our study, this is largely due to the development of water bodies within persistent swales and polygonal tundra. Scroll crests and polygon ridges possess thin SSOLs while swales and submerged polygon centers and filled with deeper SSOLs.

organics yielded a ^{14}C age of 880 yr (Table 2). This suggests that the first 1700 years of accumulated C has been lost to decomposition and/or cryoturbation. A mass balance between organic matter lost and organic matter gained through primary production at the ground surface is consistent with the steady state in SSOL thicknesses we observe along the two chronosequences.

6.4 SSOLs and Arctic Landscape Dynamics

Temperature data from retrogressive thaw slumps in the Nigu valley, from sand dunes in the Killik valley, from Smith Mountain's climax-state SSOLs, and at the Lawrence's Bend chronosequence reveal how SSOLs affect the growing season temperature regime of the mineral soil surface over the course of soil development (Fig. 15). The difference between above- and belowground growing degree days describes the air's thermal advantage over soil (Swanson et al., 2000). Following the stabilization of new geomorphic surfaces (i.e., after a disturbance that restarts primary succession), aboveground growing conditions can have either a slight thermal advantage (they are warmer) *or* a slight disadvantage (they are colder) over the mineral soil. The accumulation of any insulating soil cover (e.g., standing clumps of grass) immediately establishes the air's thermal advantage over the mineral soil and sets in motion a positive feedback leading to the accumulation of more organic material. The thermal advantage of the surface microclimate increases as soil surface organics continue to accumulate up to a thickness of about 7 cm. After this thickness is reached, the rate of increase in thermal advantage per unit increase in SSOL thickness declines (Fig. 15). In effect, any further increase in insulative effects resulting from thickening SSOLs are obviated by the increased thermal conductivity of the increasing decomposed organic material that comprises it. But note this in situations where decomposition is minimal - as in rapidly accumulating Sphagnum peat - thermal advantage probably does continue to increase linearly with organic accumulation.

The 7-cm threshold in SSOL thickness may be quite important biologically. Soil temperatures below 0°C retards most belowground decomposition, and cooling below -6°C halts even the hardiest soil microbes (Panikov et al., 2006). Our data show that 7 cm of SSOL has nearly the same biologically relevant cooling effect as 15 or 30 cm of SSOL. In other words, the greatest impacts on the mineral soil temperature regime and thus on resident microbial environment

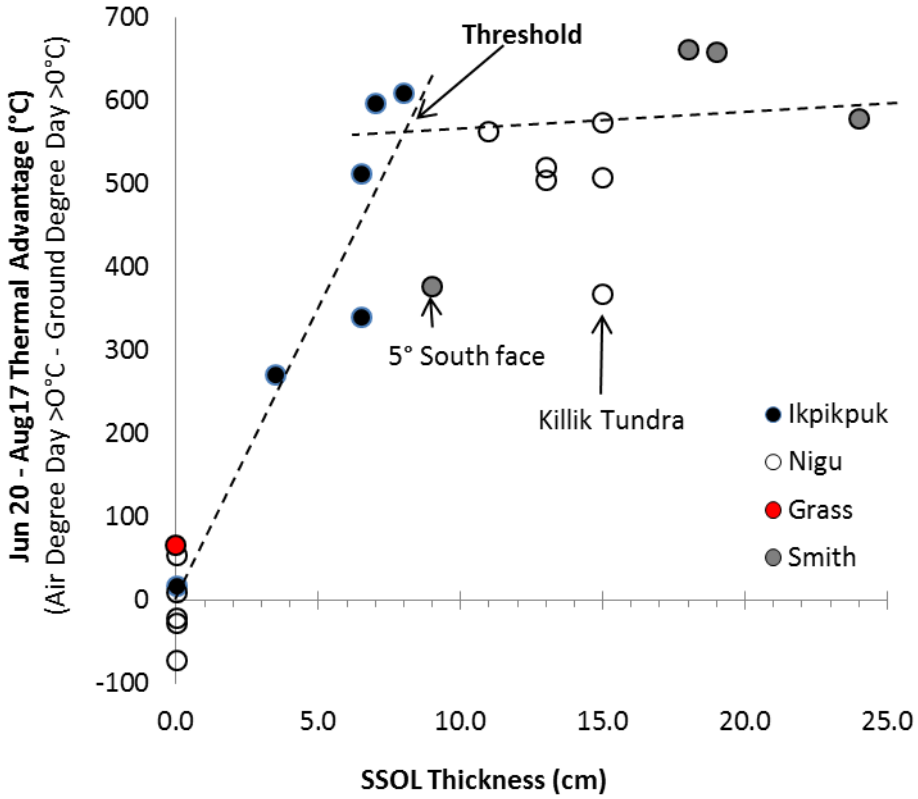

Figure 15. SSOL depth and the thermal advantage. Thermal advantage is the difference in accumulated growing degree days between the air and soil environment. Two anomalous points are marked: a south facing slope of 5 degrees and SSOL-covered sand dunes appear to have unusually small thermal advantages. This is likely due to the increased radiation found on south facing slopes and the coarse nature of sand which facilitates drainage and aeration.

occur during the first 7 cm of SSOL accumulation. Accumulation of SSOL in excess of 7 cm may be largely irrelevant to biological activity within the mineral soil.

On the other hand, accumulation of SSOLs >7 cm thick does become important when considering SSOL's role in landscape evolution. In the absence of large-scale disturbances like flood deposition/erosion or fires that are intense enough to remove entire SSOLs, what we see today is the slow accumulation of SSOLs up to some local, steady state thicknesses, accompanied by the decoupling of mineral horizons from previously important biophysical processes. In addition to becoming thermally insulated, mineral soils become physically armored to aboveground disturbances like animal digging, burning, and erosion by wind or running water. This was the case at the end of the last ice age when the accumulation of SSOLs coincided with a reduction in hillslope erosion, sediment transport, and hence alluviation in valleys (Mann et al., 2010). A return to floodplain aggradation and widespread occurrence of early successional, SSOL-free vegetation communities would require an increase in major disturbances like landslides or fire (Liljedahl et al., 2007, Mann et al., 2010).

What causes the marked inflection in the thermal-advantage curve after approximately 7 cm of SSOL thickness has accumulated (Fig. 15)? The explanation may relate to how the thermal properties of a SSOL changes as it accumulates. SSOLs more than about 7 cm thick often contain Oi, Oe, and Oa horizons, each of which is progressively more decomposed and hence has a greater bulk density (Michaelson et al., 2013). As bulk density increases, so does thermal conductivity, which lowers the insulating capacity. In effect, any insulation gained by increasing SSOL thickness is obviated by reduced insulation per unit of SSOL thickness caused by compaction and

decomposition at the base of the SSOL. This effect may determine the steady state SSOL thicknesses that are reached along the floodplain chronosequences (Fig. 10).

6.5 The Future of Arctic Soil Surface Organic Layers

Accumulation of surface organics most often occurs in lowland arctic and subarctic settings where the mean annual soil temperature is 0 °C and where above ground productivity is "thermally advantaged" over below-ground decomposition (Swanson et al., 2000). The outcome of this organic matter / thermal-advantage relationship is reflected in the initiation times of prehistoric peatlands and their subsequent accumulation rates. The initiation frequency of circumpolar peatlands peaked ca. 8,000–12,000 YBP (MacDonald et al., 2006). In Alaska, most peatlands began to accumulate between 11,000 and 9,000 YBP during the Holocene Thermal Maximum during all-time-highs in solar insolation when summers were warmer and more moist than today (Jones and Yu, 2010; Mann et al., 2010;). When these peatlands began accumulating organic matter, soil temperature regimes were probably close to the 0°C mean annual soil temperature marking the thermal-advantage threshold between net decomposition and accumulation (Swanson et al., 2000).

As climate continues to warm over the coming decades (Hinzman et al., 2005), northern Alaska could see a return of the SSOL-conducive climate regime that favored paludification during the early Holocene. At our monitoring sites, the mean annual soil temperature of bare soil surfaces was -1.5 °C. Soil temperatures at a depth of 46 cm from a nearby weather station recorded a mean annual ground temperature of -2.7 °C and -2.5 °C under moss and shrub

groundcover, respectively (GIPL, 2013). These temperatures are well below the 0°C threshold required for peat accumulation (Swanson et al., 2000). It follows that if air temperatures continue to warm, the capacity for SSOL accumulation may increase as well.

Several other considerations need to be taken into account when predicting the future of arctic SSOLs. First, precipitation during the growing season would have to remain constant or increase for SSOLs to grow further. Currently, precipitation increases are predicted mainly for the winter season, and there has been an overall negative trend in water balances (P-PET) on the North Slope since the 1960s (Hinzman et al., 2005). Second, additional SSOL accumulation will have to outpace disturbance events like thermokarst and fire. Enhanced thawing of permafrost and increased tundra fires are both predicted over coming decades (Higuera et al., 2011; Hu et al., 2010; Smith et al., 2005). These disturbance events may promote continued shrub expansion and its associated warming of soils and boosting of microbial decomposition rates (Tape et al., 2006). Is the Arctic headed towards a future of increased SSOL accumulation as soils approach the optimal mean annual soil temperature of 0°C, or will widespread SSOLs become an artifact of the past due to increased disturbance rates and changes to vegetation architecture? Answering this question will be important in determining whether the Arctic will serve as a carbon source or sink in coming centuries.

7.0 CONCLUSION

1) Topography Predicts SSOL Thickness: The *duration of direct radiation*, *up-slope-drainage-area*, *relative elevation*, and *slope angle* are the most important topographic factors influencing SSOL thickness in the Arctic Foothills. Together, these attributes explain 55% of the

variation in SSOL thickness, leaving 45% of the variation in environmental parameters currently unaccounted for. Despite this, our SSOL-thickness model still performs better than most spatially predictive, soil-distribution models developed in other regions.

2) Estimates of Belowground Carbon Stocks: Smith Mountain contains an estimated total of 0.32 ± 0.04 Tg or 6.6 ± 0.8 kg C m^{-2} within its SSOLs (± = 95% c.i.). There could be up to 1.9±0.52 Tg or 40.6±2.6 kg C m^{-2} contained in the soil to a depth of 1 meter. While SSOL-based C stocks agree with pre-existing estimates of SSOL-based carbon within the Arctic Foothills, our estimates of the C stores to 1 meter depth are probably overestimates due to the upland (i.e. rocky) nature of the study area.

3) Rates of SSOL Formation: On floodplains in the Arctic Foothills, SSOLs begin to accumulate within 5-20 years after new geomorphic surfaces are created, but they require 500-700 years to reach a mature, steady state. Note that these rates are for SSOL formation on sandy, flat, lowland surfaces. The rate of SSOL development is probably appreciably slower on steep slopes underlain by coarser parent material.

4) SSOL Feedbacks on Soil Temperature: The formation of SSOLs significantly cools underlying mineral soils. Mean annual soil temperature at the SSOL/mineral interface is reduced by 3° C, and available growing degree days (>0 °C) within the mineral soil are reduced by nearly 80%. This provides the aboveground microhabitat of primary producers with a distinct thermal advantage over the belowground microhabitat of decomposers. Based on the present-day, mean annual temperatures of bare soil surfaces, SSOL formation is primed to begin in the Arctic Foothills as soon as these surfaces stabilize after disturbances like deeply burning fires or landslides. The accumulation of any insulating, organic material on the ground surface quickly

shifts the thermal advantage to aboveground productivity and triggers the positive feedback loop favoring SSOL accumulation.

5) SSOLs and Future Warming in the Arctic Foothills: In the Arctic and Subarctic, accumulation of surface organics most often occurs when mean annual soil temperature (MAST) is around 0 °C. Because mean annual soil temperature today is < 0°C, SSOL accumulation could increase in the Arctic Foothills *if* precipitation during the growing season remains the same or increases *and if* disturbance events like thermokarst and fire do not outpace SSOL accumulation.

REFERENCES

Beringer, J., Lynch, A.H., Chapin III, F.S., Mack, M., Bonan, G.B., 2001. The representation of Arctic soils in the Land Surface Model: The importance of mosses. *Journal of Climate* 14: 3324-3335.

Blaauw, M., 2010. Methods and code for 'classical' age-modeling of radiocarbon sequences. *Quaternary Geochronology* **5**: 512-518.

Bockheim, J.G., Walker, D.A., Everett, K.R., Nelson, E.E., Shiklomanov, N.I., 1998. Soils and cryoturbation in moist nonacidic and acidic tundra in the Kuparuk River Basin, arctic Alaska, U.S.A. Arctic and Alpine Research 30: 166-174.

Bockheim, J.G., 2007. Importance of Cryoturbation in Redistributing Organic Carbon in Permafrost-Affected Soils. *Soil Science Society of America Journal* 71: 1335-1342.

Bonan G.B., Shugart, H.H., 1989. Environmental-factors and ecological processes in boreal forests. *Annual Review of Ecology, Evolution, and Systematics* 20: 1–28.Bouma, J., 1989. Using soil survey data for quantitative land evaluation. *Advances in Soil Science* 9: 177–213.

Briner, J.P., Kaufman, D.S., 2008. Late Pleistocene mountain glaciation in Alaska: key chronologies. *Journal of Quaternary Science* 23: 659-670.

Burn, C.R., Friele, P.A., 1989. Geomorphology, Vegetation Succession, Soil Characteristics and Permafrost in Retrogressive Thaw Slumps near Mayo, Yukon Territory. *Arctic* 42: 31-40.

ESRI 2011. ArcGIS Desktop: Release 10. Redlands, CA: Environmental Systems Research Institute.

French, HM. 2007. *The Periglacial Environment.* John Wiley & Sons, Ltd: Chichester. 458 pp.

Geophysical Institute – Permafrost laboratories (GIPL): http://permafrost.gi.alaska.edu/search/node/ivotuk (last accessed July, 2012), 2013.

Gessler, P.E., Chadwick, O.A., Chamran, F., Althouse, L., Holmes, K., 2000. Modeling soil-landscape and ecosystem properties using terrain attributes. *Soil Science Society of America* 64: 2046-2056.

Gessler, P.E., Moore, I.D., McKenzie, N.J. Ryan, P.J., 1995. International soil-landscape modeling and spatial prediction of soil attributes. *Journal of Geographical Information Systems* 9: 421-432.

Gorham, E., 1957. Development of Peat Lands. *The Quarterly Review of Biology* 32: 145-166.

Gorham, E., 1991. Northern Peatlands: Role in the carbon cycle and probable responses to climate warming. *Ecological Applications* 1: 182-195.

Graniero, A.P., Price, J.S., 1999. The importance of topographic factors on the distribution of bog and heath in a Newfoundland blanket bog complex. *Catena* 36: 233-254.

Hicken, E.J., 1974. The development of meanders in natural river channels. *American Journal of Science* 274: 414-442.

Higuera P.E., Chipman, M.L., Barnes, J.L., Urban, M.A., Hu, F.S., 2011. Variability of tundra fire regimes in Arctic Alaska: millennial scale patterns and ecological implications. *Ecological Application*s 21: 3211-3226.

Hinzman, L*., et al.,* 2005. Evidence and implications of recent climate change in northern Alaska and other Arctic regions. *Climate Change* 72: 251–298*.*

Hinzman, L.D., Kane, D.L., Gieck, R.E., Everett, K.R., 1991. Hydrologic and thermal-properties of the active layer in the Alaskan Arctic*. Cold Regions Science and Technology* 19: 95–110.

Hobbie, S.E., Schimel, J.P., Trumbore, S.E., Randerson, J.R., 2000. Controls over carbon storage and turnover in high-latitude soils. *Global Change Biology* 6: 196-210.

Holden, N.M., Connolly, J., 2011. Estimating the carbon stock of a blanket peat region using a peat depth inference model. *Catena* 86: 75–85.

Hu F. S., Higuera P.E., Walsh J.E., Chapman W.L., Duffy P.A., Brubaker L.B., and Chipman M.L., 2010. Tundra burning in Alaska: linkages to climatic change and sea-ice retreat*. Geophysical Research: Biogeosciences.* 115: G04002.

Intergovernmental Panel on Climate Change (IPCC), 2007. Climate change 2007: the physical science basis. Contribution of Working Group 1 to the Fourth Assessment Report of the Intergovernmental Panel on Climate Change, New York.

Johnson, K.D., Harden, J., McGuire, A.D., Bliss, N.B., Bockheim, J.G., Clark, M., Nettleton-Hollingsworth, T., Jorgenson, M.T., Kane, E.S., Mack, M., O'Donnell, J., Ping, C.L., Schuur, E., Turetsky, M.R., Valentine, D.W., 2011. Soil carbon distribution in Alaska in relation to soil forming factors. *Geoderma* 167-168: 71-84.

Jones, M.C., Yu, Z. 2010. Rapid deglacial and early Holocene expansion of peatlands in Alaska. *Proceedings of the National Academy of Sciences* 107: 7347-7352.

Lantuit, H., Polland, W.H., Couture, N., Fritz, M., Schirrmeister, L., Meyer, H., Hubberten, H.W., 2012. Modern and Late Holocene Retrogressive Thaw Slump Activity on the Yukon Coastal Plain and the Herschel Island, Yukon Territory, Canada. *Permafrost and Periglacial Processes* 23: 39-51.

Liljedahl, A., Hinzman, L., Busey, R., Yoshikawa, K., 2007. Physical short-term changes after a tussock tundra fire, Seward Peninsula, Alaska. *Journal of Geophysical Research* 112: F02S07.

MacDonald, G.M., Beilman, D.W., Kremenetski, K.W., Sheng, Y., Smith, L.C., Velichko, A.A., 2006. Rapid early development of circum-arctic peatlands and atmospheric CH_4 and CO_2 variations. *Science* 314: 285-288.

Mann, D.H., Grove, P., Reanier, R.E., Kunz, M.L., 2010. Floodplain, permafrost, cottonwood trees, and peat: What happened the last time climate warmed suddenly in arctic Alaska? *Quaternary Science Reviews* 29: 3812-3830.

Michaelson, G.J., Ping, C.L., Kimble, J.M. 1996. Carbon storage and distribution in tundra soils of Arctic Alaska, U.S.A. *Arctic and Alpine Research* 28: 414-424.

Michaelson, G. J., Ping, C. L., Clark, M., 2013. Soil Pedon C and N Data for Alaska: an analysis and update *Open Journal of Soil* Science 3: 132-142.

Mishra, U., Riley, W.J., 2012. Alaska soil carbon stocks: spatial variability and dependence on environmental factors. *Biogeoscience* 9: 3637-3645.

Molenaar, C.R., Egbert, R.M., Krystinik, L.F., 1988. Depositional facies, petrography, and reservoir potential of the Fortress Mountain formation (lower cretaceous) central North Slope, Alaska. Geology and Exploration of the National Petroleum Reserve in Alaska, 1974-82. *U.S.G.S. Professional Paper* 1399.

Nanson, G.C., 1980. Point bar floodplain formation of the meandering Beatton River, northeastern British Columbia, Canada. *Sedimentology* 27: 3-29.

National Water Information System: Web Interface, USGS Water Resources IKPIKPUK R BL FRY C NR ALAKTAK AK (http://waterdata.usgs.gov/ak/nwis/inventory/?site_no=15820000&agency_cd=USGS&)
Accessed 5-04-2013, 2013

Niu, F., Luo, J. Lin, Z. Ma, W. Lu, J., 2012. Development and thermal regime of a thaw slump in the Qinghai-Tibet plateau. *Cold Regions Science and Technology* 83-84: 131-138.

Nowacki, G., Spencer, P., Fleming, M., Brock, T., Jorgenson, T., 2001. Ecoregions of Alaska: 2001. U.S. Geological Survey Open-File Report 02-297 (Region Descriptions).

Panikov, N.S., Flanagan, P.W., Oechel, W.C., Mastepanov, M.A., Christensen, T.R. 2006. Microbial activity in soils frozen to below -39 °C. *Soil Biology and Biogeochemistry* 38: 785-794.

Parry, L.E., Charman, D.J., Noades, J.P.W., 2012. A method for modeling peat depth in blanket peatlands. *Soil Use and Management* 28: 614-624.

Ping, C.L., Bockheim, J.G., Kimble, J.M., Michaelson, G.L., Walker, D.A. 1998. Characteristics of cryogenic soils along a latitudinal transect in arctic Alaska. *Journal of Geophysical Research: Atmospheres* 103: 28917-28928.

Ping, C.L., Michaelson, G. J., Jorgenson, M.T., Kimble, J.M., Epstein, H., Romanovsky, V.E., Walker, D.A., 2008. High stocks of soil organic carbon in the North American Arctic Region. *Nature Geoscience* 1, 615 - 619.

Rieger, S., Schoephorester, D. B., Furbush, C. F., 1979. Exploratory Soil Survey of Alaska, USDA Soil Conservation Service, US Government Printing Office, Washington D.C., 1979.

Smith, L.C., Sheng, Y., MacDonal, G.M., and Hinzman, L.D., 2005. Disappearing Arctic Lakes. *Science* 308: 1429-1429.

Stuiver, M., Reimer, P.J., 1986. A computer program for radiocarbon age calibration. *Radiocarbon* 28: 980–1021.

Swanson, D.K., Lacelle, B., Tarnocai, C., 2000. Temperature and the boreal subarctic maximum in soil organic carbon. *Géographie physique et Quaternaire* 54: 157-167.

Tape, K., Sturm, M., Racine, C., 2006. The evidence for shrub expansion in Northern Alaska and the Pan-Arctic, *Global Biological Change* 12: 686-702

Tarnocai, C., Canadell, J.G., Schuur, E.A.G., Kuhry, P., Mazhitova, G., Zimov, S., 2009, Soil carbon pools in the northern circumpolar permafrost region. *Global Biogeochemical Cycles* 23: GB2023.

Tsai, C.C., Chen, Z.S., Duh, C.T., Horng, F.W., 2001. Prediction of soil depth using soil-landscape regression model: a case study on forest soils in Southern Taiwan. *Proceedings of the National Science Council,* ROC(B) 25: 34-39.

Van Cleve, K., Chapin III, F.S., Flannagan, P.W., Viereck, L.A., and Dyrness, C. T., 1986. Forest Ecosystems in the Alaskan Taiga. Springer-Verlag, 230 pp.

Walker, D.A., 2000. Hierarchical subdivision of Arctic tundra based on vegetation response to climate, parent material and topography. *Global Change Biology* 6: 19-34.

Walker, D.A., Bockheim, J.G., Chapin III, F.S., Eugster, W., Nelson, F.E., Ping, C.L., 2001. Calcium-rich tundra, wildlife, and the "Mammoth Steppe." *Quaternary Science Reviews* 20: 149-163.

Walker, M.D., Walker, D.A., Everett, K.R., Charles, S., 1989. Wetland Soils and Vegetation, Arctic Foothills, Alaska. US Fish and Wildlife Biological Report 89 (7). 92 pp.

Walker, M.D., Walker, D.A., Auerbach, N.A., 1994. Plant communities of a tussock tundra landscape in the Brooks Range Foothills, Alaska. *Journal of Vegetation Science* 5: 843-866.

Zuur, A.F, Leno, E.N., Elphick, C.S., 2010. A protocol for data exploration to avoid common statistical problems. *Methods in Ecology and Evolution* 1: 3-14.